ELSEVIER

Nuclear Engineering and Design 184 (1998) 239–252

Nuclear Engineering and Design

Evaluation of pulsed laser holograms of flashing sprays by digital image processing and holographic particle image velocimetry

O. Feldmann [a,*], E.h.F. Mayinger [a], P. Gebhard [b]

[a] *Chair A for Thermodynamics, Technical University of Munich, 85747 Garching, Germany*
[b] *Audi AG, Technische Entwicklung, Abteilung: Versuch Gesamtfahrzeug, Ingolstadt, Germany*

Received 3 March 1998; accepted 3 March 1998

Abstract

The present paper deals with the analysis of the disintegration process of both subcooled and superheated sprays generated in a flat spray nozzle. Both the macroscopic structures of a spray, such as the breakup-length and the spray-angle, and its microscopic structures, such as the number, the size, the location, and the velocities of the generated droplets as a function of varying injection conditions have been investigated. The short time holography has been applied as the measuring technique. Two holograms of the generated spray are taken simultaneously which results in two three-dimensional (3-D) reconstructions of the spray, seen from different directions. Computer based algorithms have been developed to determine the quantities to be measured that are stored on the holograms. A stereo-matching module correlates both views and determines the position and/or the velocity of each droplet. The applicability of the employed holographic technique and of the filtering and correlating modules is proven by the presented results.

1. Introduction

In many technical applications sprays play an important part. Sprays can be formed by:

- mechanical disintegration of the liquid due to shear forces and induced turbulence,
- and thermodynamic disintegration by flashing of the liquid.

Especially in the field of fuel injection and with respect to safety aspects in process engineering, the disintegration of a liquid jet by flashing is an interesting phenomenon. This paper reports on a study of sprays generated by injecting subcooled or superheated liquid through flat spray pressure nozzles. When superheated liquid is injected, its fragmentation is caused by both the mechanical forces and the growing of vapor bubbles in the metastable part of the liquid veil. By applying the short time holography, the conditions in the measuring volume are recorded three-dimensionally (3-D) during the very short exposure time of only a few nanoseconds. The holograms contain the information about macroscopic structures such as

* Corresponding author. Tel.: +49 89 28916230; fax: +49 89 28916218; e-mail: feldmann@thermo-a.mw.tu-muenchen.de

0029-5493/98/$ - see front matter
PII S0029-5493(98)00200-3

the break-up length and the spray angle of the liquid veil near the nozzle and microscopic structures such as the size, the position, and the velocity of the droplets further downstream. The recorded holograms are reconstructed by means of a continuous laser beam and observed by using a microscope lens mounted on a CCD-camera. The obtained images are transferred to an image processing system. The main problem which appears in the evaluation of holograms consists in selecting and classifying well-focussed particles while the CCD-camera scans the 3-D holographic image. In the last 15 years, many efforts have been made to evaluate short time holograms of particle fields by applying techniques of the digital image processing. An introduction to this problem was presented by Hausmann and Lauterborn (1980). This paper presents two computer aided procedures to evaluate short time off-axis holograms of sprays (single and double pulsed holograms, respectively) and to reconstruct the spray and its velocity field three-dimensionally on a computer. They are based on techniques of the digital image processing (IP) and the particle imaging velocimetry (PIV). When using these procedures, the operator is released from the situation of taking decisions interactively during the evaluation process. This allows a more efficient application of drop focussing and classifying criteria which results in a substantial increase of the measurements' accuracy and in an effective reduction of the time that is necessary to evaluate the holograms.

2. Experimental facility

The experiments have been carried out in the test facility illustrated in Fig. 1. After the test fluid has been degassed by an ultrasonic treatment and by boiling, it is stored in a pressurized reservoir. The pressure in this reservoir can be varied between 0.1 and 2 MPa by means of nitrogen. Three electrical heaters, with an electrical output of 1.2 kW each, can be applied to heat the liquid. From an outlet in the lower part of the vessel, the fluid is pumped through an oil heated heat exchanger for a fine adjustment of its temperature and then to the nozzle. The test section itself consists of the nozzle and a coflowing vertical wind tunnel which is capable of providing air velocities up to 50 m s^{-1} and temperatures up to 600°C. The test section has been designed for atmospheric pressure and is made of a glass-octagon with an inner diameter of 300 mm and a height of 250 mm in order to allow an optical access. The nozzle, which is located concentrically with respect to the surrounding air flow, can be moved axially in order to allow the observation of any section of the generated spray. Downstream of the test section, the mixture of air, test fluid, and vapor is cooled down in a heat exchanger. The condensate is separated in a demister and collected. Measurements of the temperature and the pressure at different points of interest in the facility have been carried out by using conventional thermocouples and pressure sensors which are monitored by a personal computer.

3. The holographic technique

The short time holography, applied in this work, represents one of the more suitable non-invasive measuring techniques in the analysis of transport phenomena (e.g. heat and mass transfer) in dispersed transparent flows. The word holography is rooted in the Greek language and describes the ability of this measuring technique to record the totality of the light information scattered by or reflected on an object, namely both, the amplitude, the intensity, and the phase distribution. Three-dimensional pictures of the entire volume of interest are taken. Due to the short exposure time, even fast-moving particles are imaged sharply. A deeper insight into this technique can be found in the literature (Leith and Upatnieks, 1964; Kiemle and Röss, 1969).

3.1. Recording of the holograms

The optical setup which has been applied to record the holograms in this study is shown schematically in Fig. 2. Two 3-D images of the generated spray, perpendicular to one another, have been taken simultaneously. Therefore, a pulsed

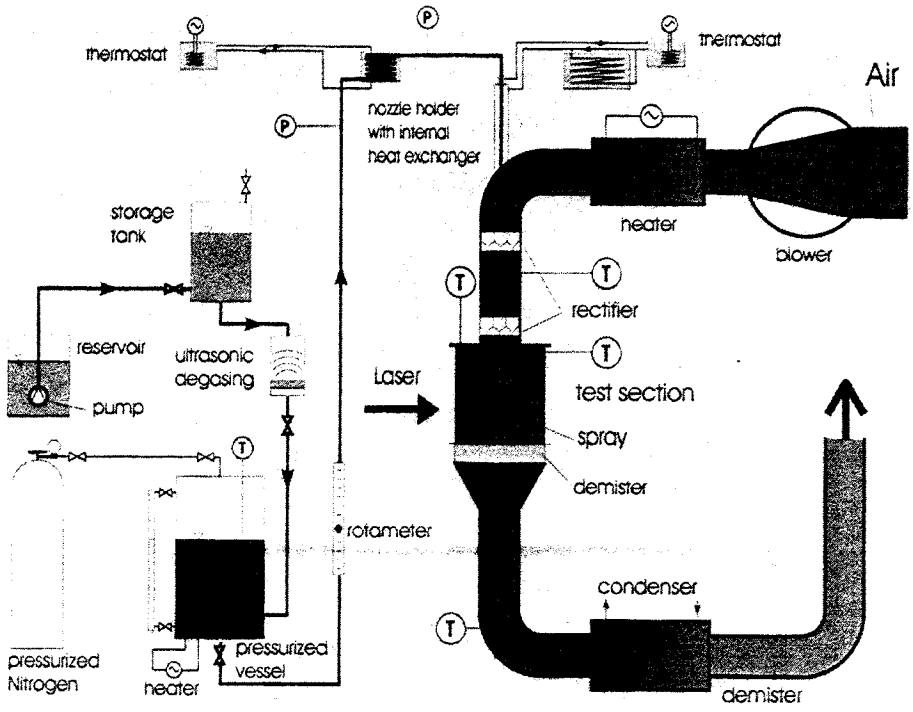

Fig. 1. Test facility.

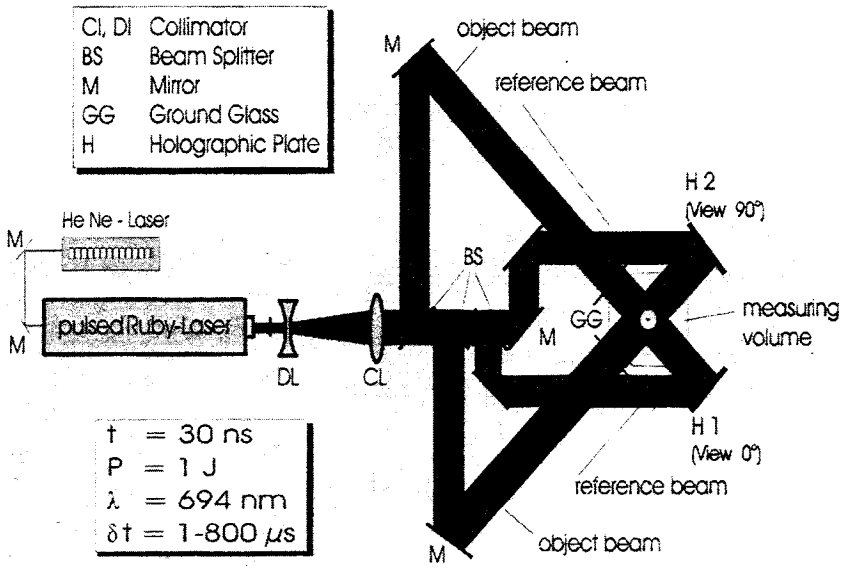

Fig. 2. Optical setup of the holographic camera.

ruby-laser which generates light pulses with an energy of 1 Joule for the very short time of 30 ns and a wavelength of 694 nm has been applied. The emitted laser beam is collimated by passing two lenses (DL, CL) and it is then split into two object beams and two reference beams in the bank of beamsplitters (BS). The object beams are diverted at the mirrors in such way that they cross the test section perpendicular to one another after they have been converted into diffuse light at a plate made of ground glass. Exiting the test section, the object beams fall perpendicularly onto the holographic plates. Contrary to that, the reference beams are diverted directly onto the holographic plates (Fig. 2). The superposition of the object beam and the reference beam results in an interference figure that contains the entire optical information and that is stored on the holographic plate.

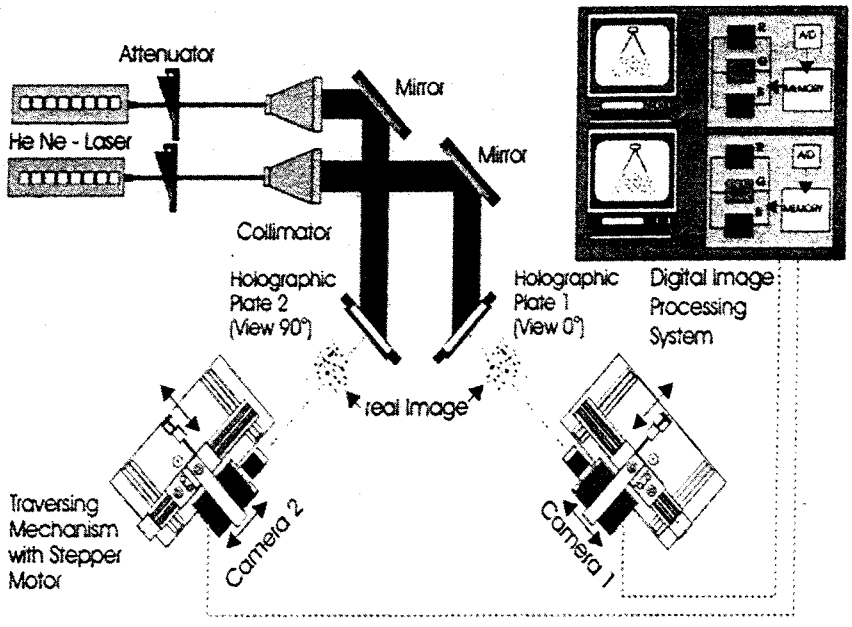

Fig. 3. Optical setup for the reconstruction and scanning of the holograms.

The laser can be operated either in a single pulse or in a double pulse mode. In a single pulse mode, the resulting holograms contain both, the macroscopic information about the geometry of the spray, the break-up of the liquid sheet, and the microscopic data, such as the droplet diameter and the spatial droplet distribution in the control volume. In addition to that, the information of the velocities and trajectories of the droplets is obtained by operating the laser in a double pulse mode. In this case, two successive conditions of the spray are recorded on each holographic plate. With the knowledge of the pulse separation, which can be varied from 1 to 800 μs, and the measured distance between the two successive images of one droplet, the velocity of each droplet is calculated.

When applying this measuring technique, particles with a diameter greater than ten times the wavelength of the laser light are imaged sharply. This results in two 3-D images of the spray, recorded simultaneously, without any restriction to the depth of the focal range. The principal features of this measuring technique are explained in a more detailed way in the literature (Chávez, 1991; Mayinger, 1994; Gebhard and Mayinger, 1995; Gebhard, 1996).

3.2. Reconstruction of the holograms

Each hologram is reconstructed by illuminating the holographic plate with a continuos HeNe-Laser beam with a wavelength of 632 nm that is simulating the reference beams during its recording with respect to the geometry and to the angle of incidence. This laser beam is diffracted at the interference figure that is stored on the holographic plate. As a result of this diffraction, the object beam which contains the entire information of the test section is obtained. A stationary image, the real image of the recorded scene, is formed three-dimensionally and distortionless in front of the holographic plates, as it is shown in Fig. 3. The dimensions of this image are scaled down with the ratio of the wavelengths of the HeNe-laser and the Ruby-laser. The optical information contained in this reconstructed image is scanned by a Newicon CCD-camera and transmitted to a digitizer. The signal is transformed into digital information and it is then stored in the digitizer frame memory in form of an array of 512×512 pixels of 8 bits. A bus interface connects the digitizer to the host computer. The processing of the digitized picture is then carried out by the host computer that uses the digitizer frame memory interactively for pixel allocation. In order to visualize the information stored in the digitizer frame

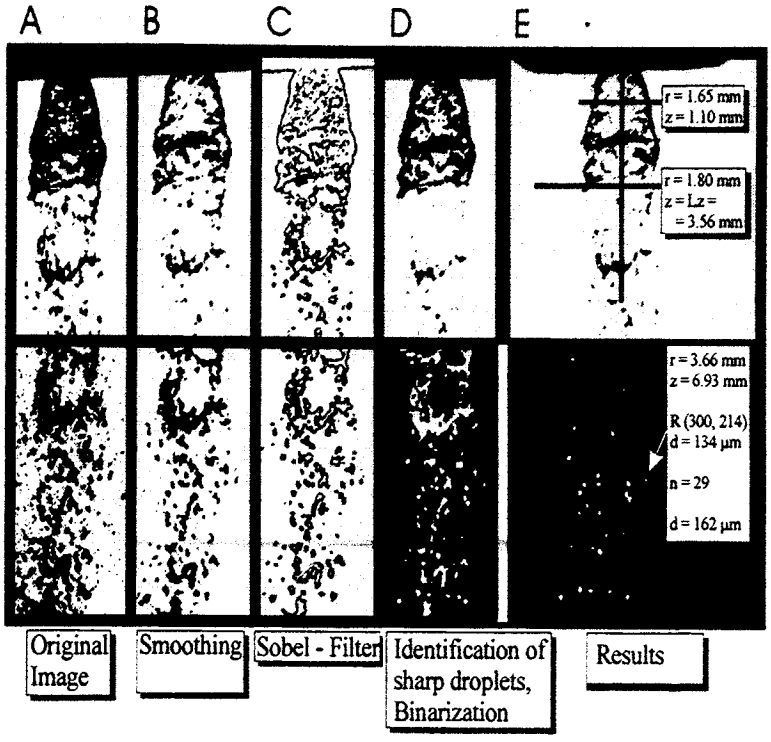

Fig. 4. Representative steps of image processing of a slice cutted from a holographic reconstruction.

memory, it produces a continuous false color RGB output signal which can be seen on the graphics monitor (Fig. 3).

The fact that the CCD-camera can only take two-dimensional (2-D) images, which is its optical plane, serves to evaluate the 3-D information which is contained in the reconstruction. The camera is equipped with an objective with a small focal range, so that only those droplets are imaged sharply which are reconstructed within the focal range of the observing camera. By moving the camera stepwise along its depth coordinate, the entire 3-D information contained in the holographic reconstruction is scanned. With a depth of focus of 2 mm, the field of view of the camera is 4×4 mm^2. The test section is divided into several subvolumes with the dimension of $4 \times 4 \times 2$ mm^3 which correspond to the field of view and the depth of field of the observing cameras. In this manner, the 3-D holographic reconstructions are transformed into a series of 2-D video images. In order to control the position of the camera it is mounted on a traversing mechanism, which is controlled by a personal computer.

Both holograms are reconstructed and evaluated as described above, so that two views of the spray perpendicular to one another are obtained. They represent two 3-D images corresponding to one 'frozen' scene of the spray, as it is illustrated in Fig. 3.

4. Evaluation of the holograms

One of the principal problems which appear in the application of short-time holography consists in dealing with the large amount of information stored in the holograms. Theoretically, holographic materials are able to store the information about the position, the texture, and the brightness of more than 10^6 particles per mm^2. Though in this study the droplet concentration was much lower (less than 10 droplets per mm^3), one single hologram can still contain the information about the position, the size, and the velocity of thousands of droplets. Comprehensive studies of the characteristics of the droplets and the interactions with their gaseous environment necessarily require the help of computer-aided particle counting and measuring methods.

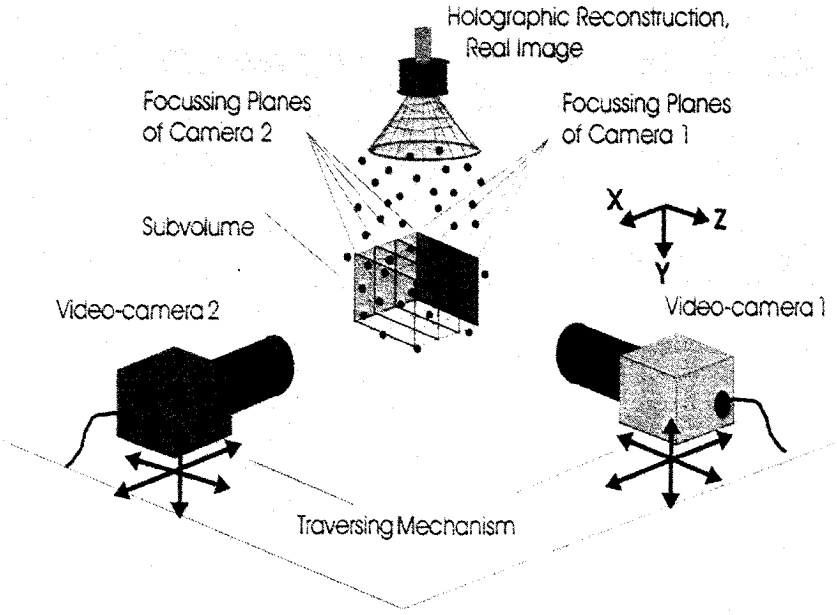

Fig. 5. Physical model of the stereomatching.

4.1. Single pulsed holograms

Representative stages of the image processing are presented exemplarily in form of photographs in Fig. 4 (Chávez, 1991). The nozzle is included for better orientation. The first module of the software transforms the original image (A) which is seen by the video-camera, into a binary image. This original image of a holographic reconstruction is smoothed (B) and treated with a gradient filter (C). Sharply imaged structures are detected, edged and filled. Finally the image is binarized (D). An additional tool in this module allows the analysis of either the big structures, such as the liquid veil (E, above) or of only the smaller structures, such as the droplets (E, below). These procedures are performed by stretching the histogram of the gray values of the image and by the application of gradient filters and threshold filters with threshold values obtained from that histogram. As a result, binary images are obtained. These images are the basis for the following evaluation algorithms. During the calibration of the optical system it has been observed that the radial and the tangential error of distortion of the used microobjective lenses (Nikon 105 mm) is less than one single pixel on the surface of the camera chip. This error is assumed to be negligibly small. A comprehensive description of hologram evaluations by applying digital image processing can be found in Chávez and Mayinger (1992).

In order to reconstruct the recorded spray three-dimensionally from the video images, the images of both views of the spray have to be correlated. The droplets differ in size and shape, but this feature-based matching is a weak criterion to correlate both views because of the influence of the illumination and the variation of the droplets' shape between both views. Generally, if this feature-based matching criterion is applied, more than two views are necessary to determine the particles' positions sufficiently accurately due to the large number of ambiguities (physically possible matches). Therefore, a second module, the stereomatching algorithm, has been developed in order to be able to perform the matching with only two views. It determines the droplets' positions in space from the binary pictures by applying the focussing criterion. The physical model used in the stereomatching process is illustrated in Fig. 5. As explained above, the depth coordinate of a droplet in one view is known within the small range of the depth of field of the observing camera. With the correspondence of the vertical coordinate of each droplet in both views, this is the second criterion required in order to determine the exact position of the droplet in the second view, since the depth coordinate in the first view is the horizontal coordinate in the second view.

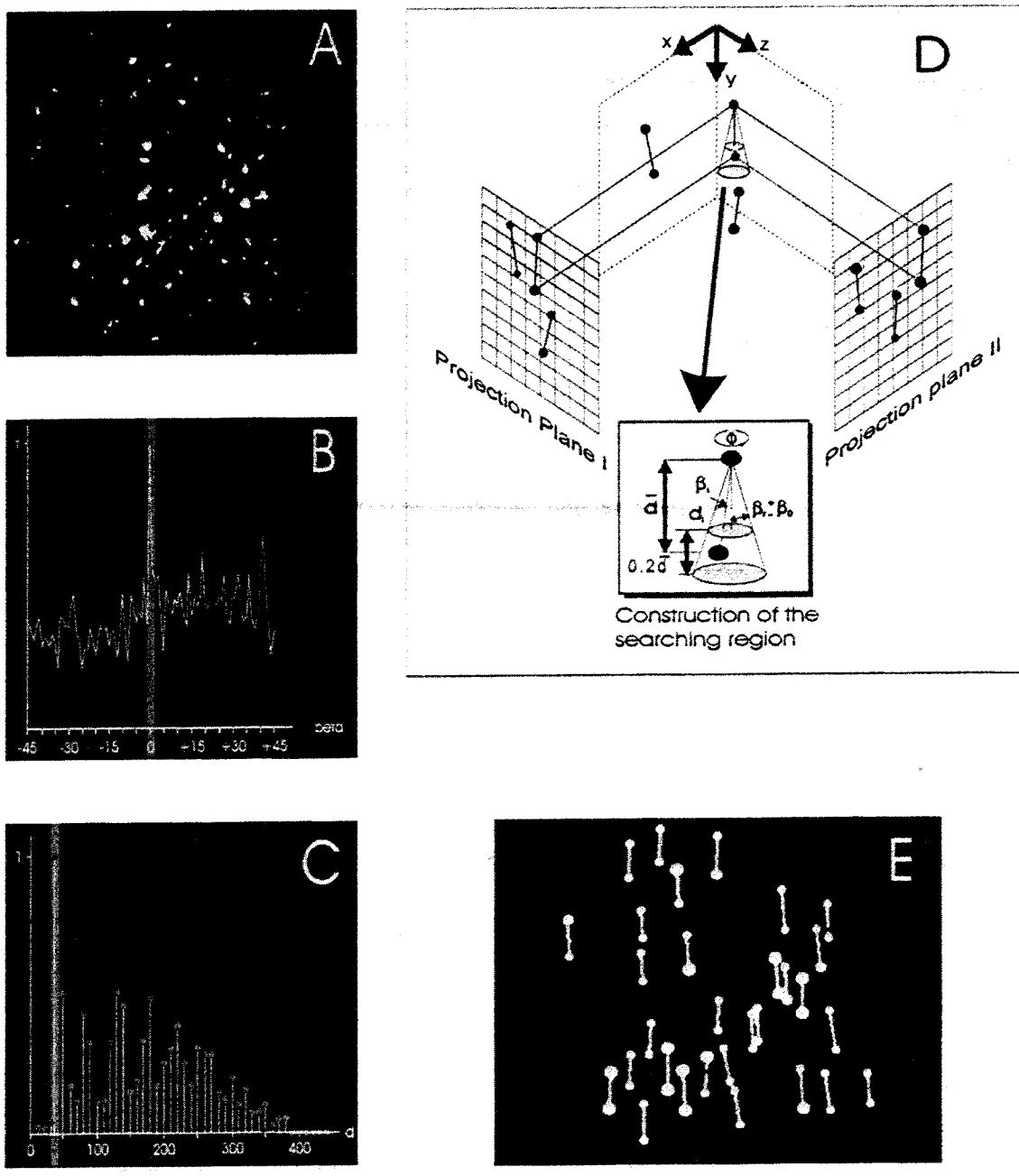

Fig. 6. The modules of the routine VEL.

4.2. Double pulsed holograms

The information about the droplets' velocities and trajectories is obtained from double pulsed holograms. The holograms contain a conglomeration of spot couples. Each couple represents one spray droplet which is imaged twice at two successive positions corresponding to the time interval ($\Delta t = 1-800$ μs) between the two exposures to the laser light. In order to evaluate the double pulsed images, a routine VEL has been developed. Its task is to identify the spot couples from the pictures taken by each camera and to measure the distance between the center points of the two images. Furthermore, it computes the droplets' trajectories related to the focussing plane of the observing camera, without considering the particles' off-plane velocity. The routine consists of two modules: a spatial frequency analyzer and a measuring algorithm. The different steps of the evaluation of double-pulsed holograms by applying the modules of the routine VEL is illustrated in Fig. 6. Firstly, the image is binarized as described above. With the assumptions that the

image was obtained from a double-pulsed holographic reconstruction, and that the depicted elements (Fig. 6A) represent droplets which are moving along the vertical axis within a guessed angle of $\pm 45°$, the first module recognizes automatically the two positions of each droplet regardless of its shape. The vectorial distance $\vec{d}$ between the two center points of each two droplets is calculated. This distance $\vec{d}$ can be split into a distance d and an angle β towards the vertical. Then a Fourier-analysis based frequency analysis converts the spatial distribution of β into a normalized frequency distribution with the maximum F_{max} used as a norm (Fig. 6B). With the information of this preferential angle, a second frequency analysis with the distance d as the independent variable is carried out (Fig. 6C). The preferential angle β_p and the preferential distance d_p appear as peaks in the diagrams. The mean velocity $\vec{v}$ is calculated from these values and the pulse separation. This algorithm is applied to both views and an average velocity projected into the focal planes of the cameras is obtained. By evaluating the mean velocities $\vec{v}$ in both views, the real angle in space, called β_r which consists of an cylinder coordinate Φ and the angle β_r is calculated. In order to determine the real velocity in space, a second module has been developed for the subroutine VEL. Both the magnitude d_p of $\vec{v}$ with a tolerance of $\pm 0.1\ d_p$ and its corresponding angle β_r with the tolerance of $\pm \beta_0$ that can be varied between 7 and 15° were incremented. The chosen tolerances allow strong variations of the droplet trajectories. When using these variations the algorithm creates a search volume to find the second position of a droplet (Fig. 6D). Herein, v_i and β_i are the real magnitude and direction of the velocity which correspond with the imaged positions of the droplet, respectively. At least 75% of the couples are detected and measured by applying the modules of the subroutine VEL (Fig. 6E). The trajectories that are obtained by applying both modules of VEL for the droplets of a spray generated by a hollowed cone nozzle are shown in Fig. 7. This algorithm works highly reliably because of the found unidirectional flow of the droplets with respect to the analyzed volume.

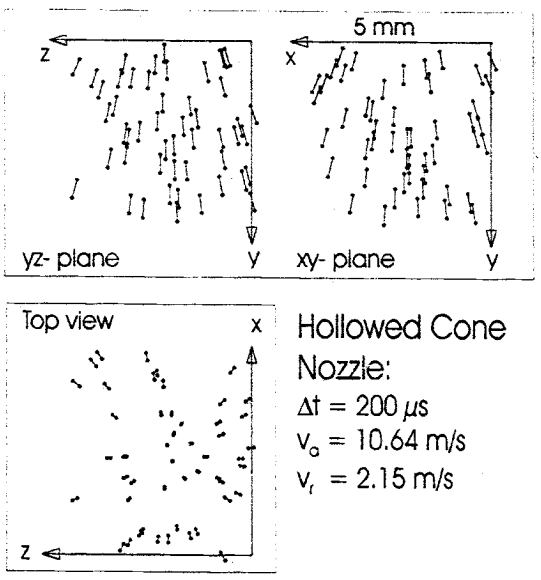

Fig. 7. Trajectories of the droplets of a spray formed in a hollowed cone nozzle.

5. Results and discussion

As an example of the applicability of the discussed recording and evaluation technique, the results obtained at a flat spray nozzle with an elliptic orifice (main axis: 1.19 mm, 0.49 mm) are presented in the following. The injection pressure of the test fluid-distilled, degassed water-ranged from 0.025 to 0.8 MPa and the temperature from 20 (subcooled liquid) up to 150°C (superheated with respect to the pressure in the test autoclave of 0.1013 MPa, (Gebhard, 1996).

5.1. Mechanism of the disintegration

Holographic reconstructions of a superheated injection jet and their binarized images are shown exemplarily in Fig. 8 for different injection conditions. By means of these images the two driving mechanisms of the disintegration of a superheated liquid jet can be explained: the sheer stress between the liquid and the adjacent gaseous phase, and the evaporation of the liquid. In case of a superheat of up to 10 K, transient sheer stresses cause oscillations increasing in amplitude along the liquid veil. These oscillations lead to the separation of unstable ligaments which disintegrate into stable droplets further downstream (A). At

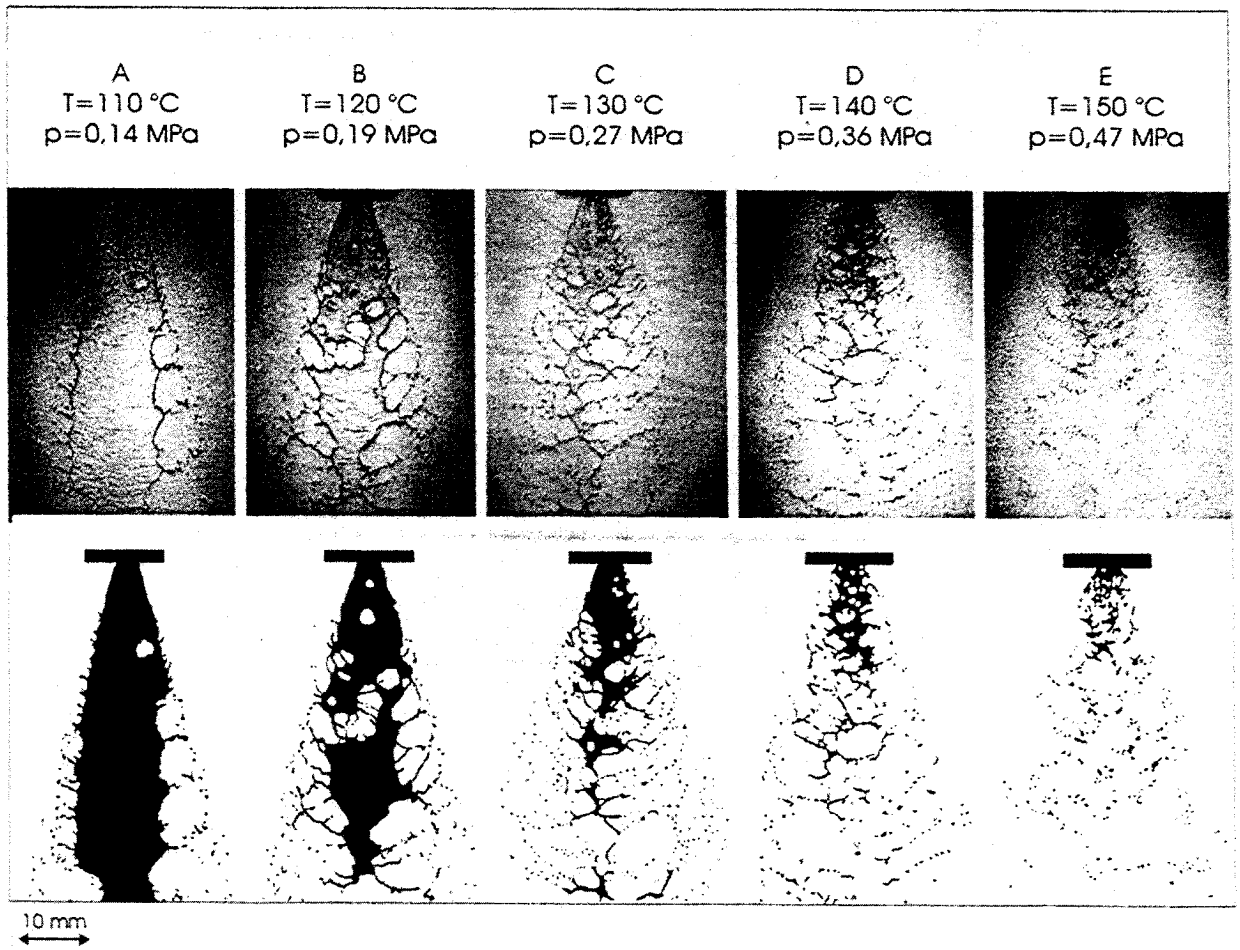

Fig. 8. Influence of different injection conditions on the spray.

this low superheat, the activation rate of nuclei is not high enough yet to have a noticeable influence on the disintegration process. The augmentation of the superheat results in a higher activation rate of these heterogenous generated nuclei. These nuclei form growing vapor bubbles causing perforations in the veil. Due to surface tension forces, these perforations grow with the distance from the nozzle which entails the separation of ligaments. These ligaments disintegrate independently from the remaining veil (B, C). If the superheat exceeds 40 K, the very high activation rate of the nuclei results in an immediate flash evaporation of the liquid exiting the nozzle (D, E).

5.2. Macroscopic structures

The shape of the liquid veil is characterized by the breakup length L_z and the spray angle α. It determines the size, the distribution, and the velocity of the generated droplets. A spray can be subdivided into three zones:

- the continuous liquid veil zone, formed by the test fluid exiting the nozzle,
- the breakup zone, where the veil is disintegrated and the droplets are generated,
- and the droplet zone itself.

The breakup length L_z, i.e. the distance between the nozzle and the breakup zone, is plotted versus the injection pressure for different temperatures in Fig. 9A. Subcooled conditions are represented by solid lines, superheated conditions are represented by dashed lines. For subcooled conditions, L_z increases with the pressure. Having reached a maximum it decreases again. The liquid is disintegrated due to the sheer stress as explained above. By increasing the temperature the viscosity and the surface tension of the liquid are decreased.

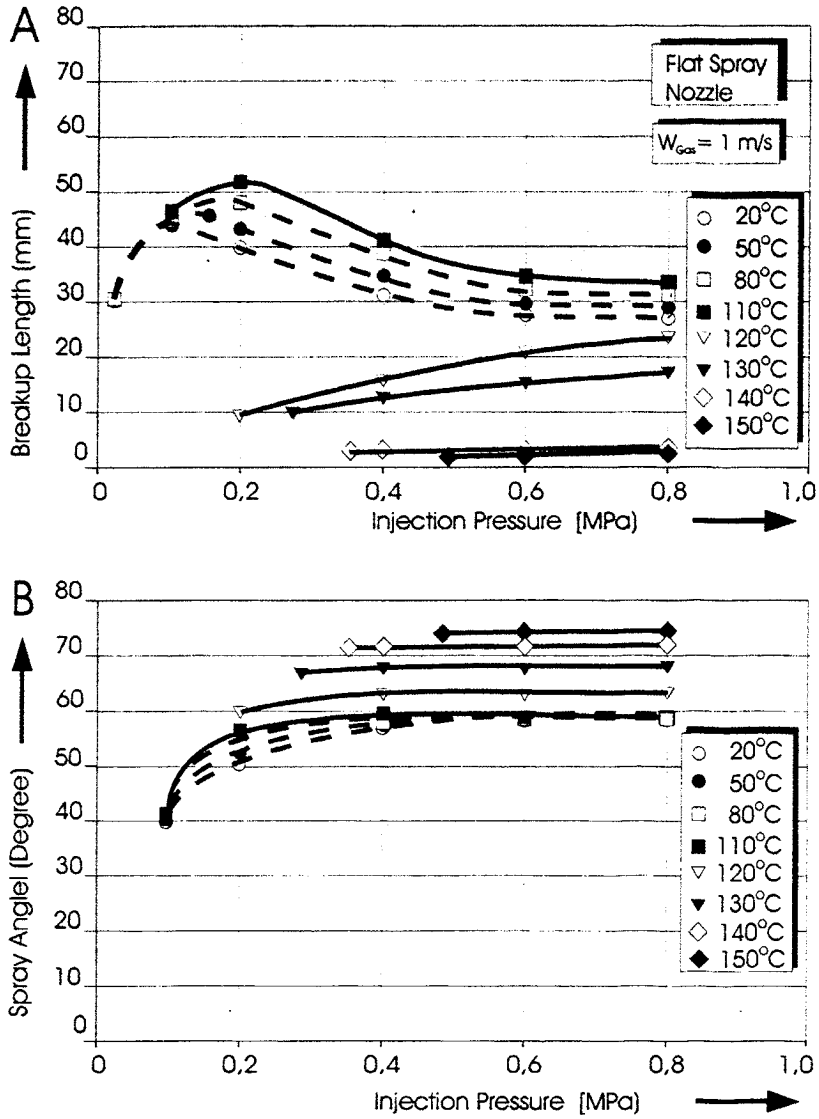

Fig. 9. Breakup length and spray angle as a function of the injection pressure for different temperatures of the test fluid.

This results in an increase of the breakup length. The appearance of slightly superheated spray is similar to those of subcooled sprays. An increase of the pressure leads to a higher velocity and greater sheer stress. Therefore the breakup length decreases in the high pressure range. In the range of ~120–130°C, the breakup length increases with the injection pressure due to the higher initial velocity of the liquid. Rising the temperature enhances the activation rate of the nuclei. This leads to in a decrease of the breakup length. If the injected liquid is highly superheated, the veil disintegrates directly after it has exited the nozzle. In this case, the breakup length L_z is not a function of the pressure.

The spray angle α is depicted versus the pressure for different temperatures of the injected liquid in Fig. 9B. For subcooled injection (dashed lines), the spray angle α increases with the injection pressure and reaches a borderline asymptotically. The influence of the temperature on the spray angle is small for injection pressures up to 0.4 MPa and negligible for higher injection pressures.

In contradiction to that, the spray angle is highly dependent on the temperature for superheated liquid. Higher injection temperatures cause an increase of the spray angle owing to the enhanced activation rate of the nuclei and thus the stronger flashing of the injected liquid.

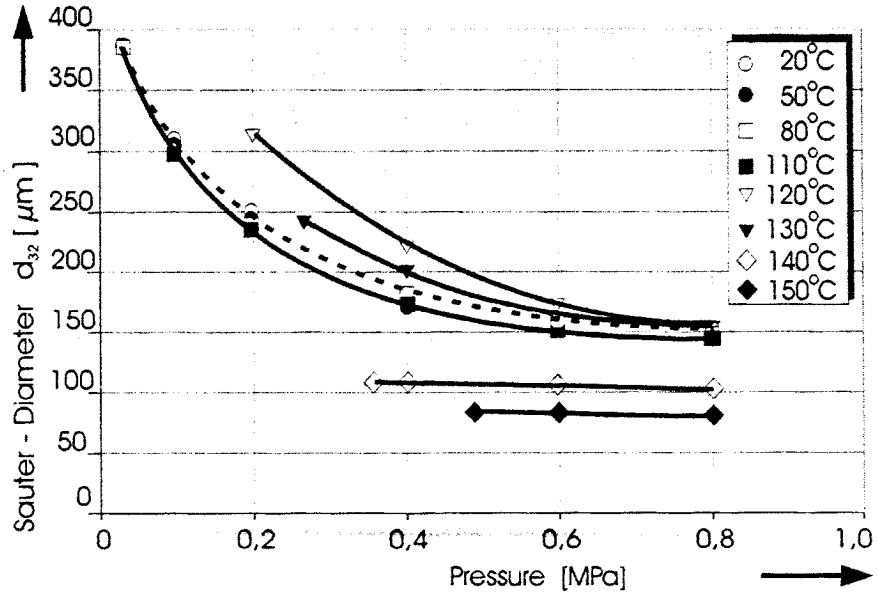

Fig. 10. Sauter-diameter as a function of the injection pressure for different temperatures of the test fluid

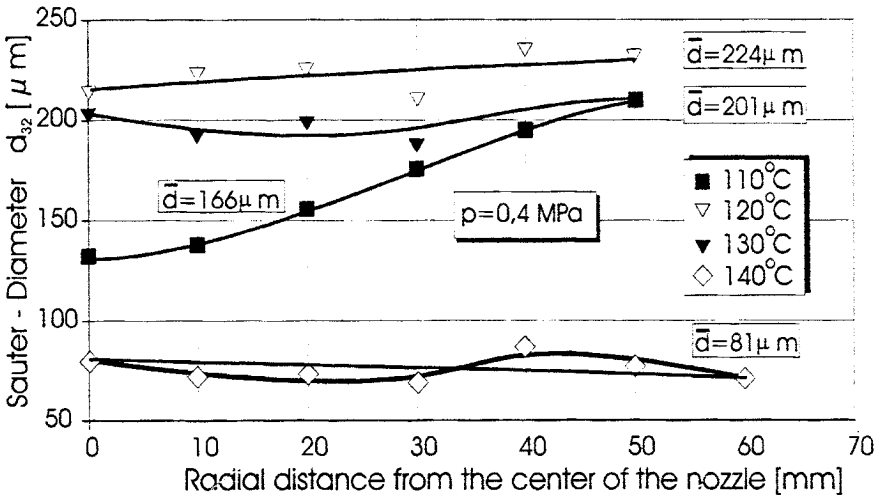

Fig. 11. Sauter-diameter as a function of the radial distance from the center of the nozzle.

5.3. Microscopic structures

From the analysis of the macroscopic structures of the different sprays it can be inferred that for any injection condition the disintegration process is completed at an axial distance of $y = 80$ mm from the orifice. Therefore, the results of the analysis of the sprays' microscopic structures which are presented in the following refer to that y-coordinate. The found diameter of the droplets is expressed by the Sauter-diameter as a function of the injection pressure for different temperatures in Fig. 10. If subcooled or slightly superheated water is injected, the droplets' Sauter-diameter strongly decrease with a higher injection pressure. An increase of the injection pressure to more than 0.6 MPa does not affect the Sauter-diameter remarkably. An increase of the pressure results in a higher velocity of the liquid and thus in higher inertial forces and sheer stresses on the veil which results in its better disintegration. For higher temperatures in the subcooled region and for slightly superheated liquid, the size of the droplets decreases because of the lower viscosity of the liquid.

For a superheat of more than 10 K, the generating of vapor bubbles becomes the governing effect of the disintegration process of the liquid

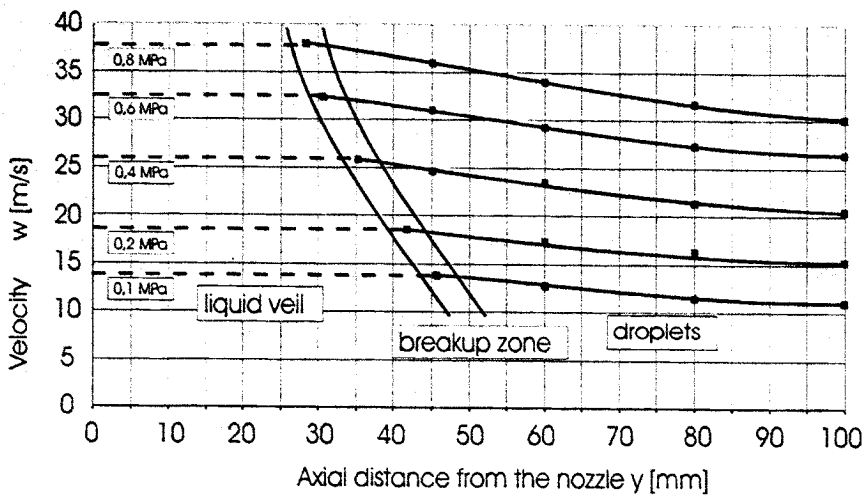

Fig. 12. Velocity of the liquid veil and the droplets of a subcooled injection jet.

veil. In the temperature range from ~110 to 130°C the separation of the ligaments from the veil can be observed. In this temperature range, the liquid sheet in the breakup zone and thus a separated ligament is thicker than the wavy sheet obtained by injecting subcooled water. This results in an increase of the Sauter-diameter of the generated droplets. If the injected liquid is highly superheated, the jet is flashed into the test section. A fine spray with a small Sauter-diameter of the generated droplets is obtained. This effect can be enhanced by a further increase of the temperature of the liquid. In this temperature range, the influence of the injection pressure on the Sauter-diameter is negligibly small.

The radial distribution of the droplets' diameter 80 mm downstream of the orifice is given in Fig. 11 for an injection pressure of 0.4 MPa. As it can be inferred from that figure, the increase of the temperature of the liquid leads to a more uniform distribution of the diameter of the generated droplets. In Fig. 12, the velocity of a subcooled jet is plotted versus the axial distance from the orifice for different injection pressures and a constant temperature of the injected liquid of 50°C. The velocities were derived from the evaluation of double-pulsed holograms as it was explained before. The velocities of the liquid veil were determined by measuring the displacement of specific characteristics in the veil. As it can be seen in Fig. 12, the veil's velocity increases and its length decreases with the injection pressure. Its velocity is constant within the range of ± 5%. When the droplets are generated, their velocity decreases with the axial distance due to the friction. The smaller droplets which were generated at high injection pressures tend to decelerate faster and to lose a higher percentage of their initial velocity than the bigger droplets which were generated at low injection pressures. The velocities of the droplets of a superheated spray have been determined at an axial distance of $y = 80$ mm downstream of the nozzle. They are plotted—classified in two diameter classes—for four radial locations in Fig. 13. The velocity of the droplets decreases with the radial distance from the center due to the higher impact of friction. Bigger droplets have a higher speed than smaller droplets because of their higher inertia. The average velocity of the droplets is also shown in Fig. 13 in form of a solid line to illustrate the loss of velocity of the droplets compared to that of the liquid veil.

5.4. Accuracy

The main source of uncertainty of this measuring technique was found to be the pixel representation of circular objects (droplets), especially if these objects are represented by less

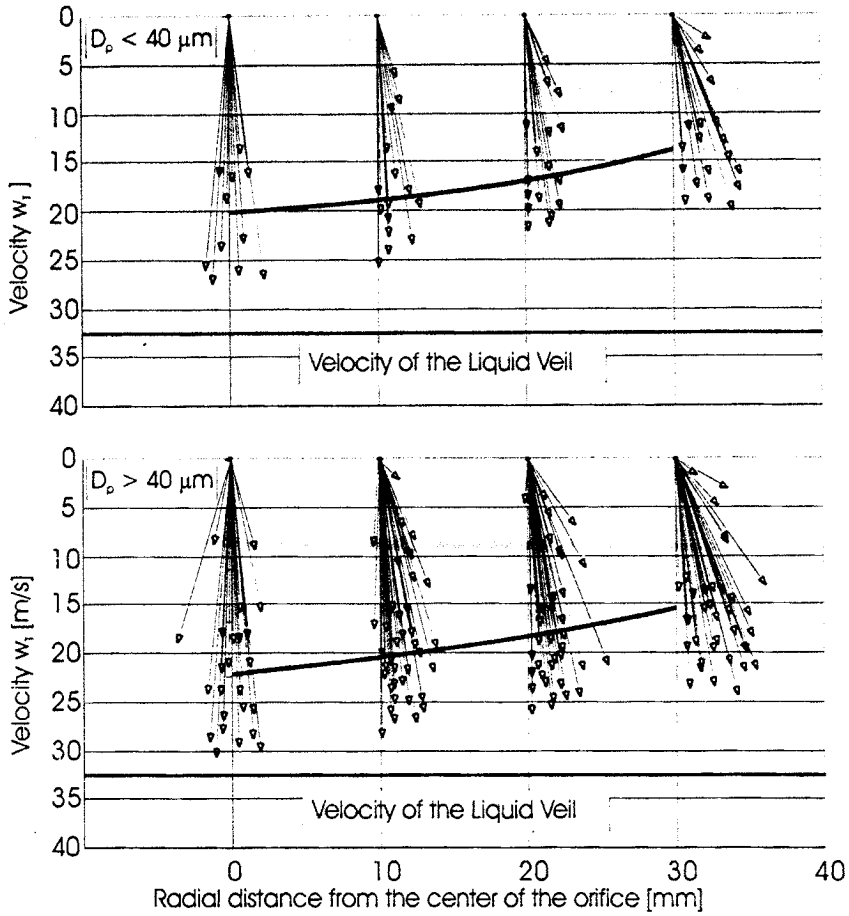

Fig. 13. Velocity of different droplet classes at an axial distance of 80 mm from the nozzle.

than 10 pixels (independent of the absolute pixel size). The resolution of the area measurement tool in the developed code was set to 5 pixels, which results in the maximum error of $\pm 3\%$ for areas with sizes between 6 and 40 pixels. In this work, the sizes of the droplets' images ranged between 14 pixels (∅ 30 µm) and 148 pixels (∅ 310 µm) pixels. The error in imaging larger objects or structures was found to be less than 1%. The determination of the velocity of one droplet depends on the quality of the stereomatching and the yield of the found couples. The fact that thousands of droplets are considered, allows the determination of their mean velocity with the high accuracy of $\pm 5\%$.

6. Conclusion

The presented 3-D particle imaging velocimetry technique is based on the evaluation of short-time holograms. The large amount of data, stored on a hologram, can be analyzed correctly without previous knowledge of the flow in the measuring volume. The code works with the high accuracy of $\pm 3\%$ for the determination of the droplets' sizes and $\pm 5\%$ for the determination of their mean velocity. It can be integrated into a digital image processing system with common digitizers (512 × 512 pixels, 8 bit depth). The application of this technique allows the analysis of both the macroscopic structures, such as the dimension of the liquid sheet, and the microscopic structures such as the droplets' sizes and velocities.

Acknowledgements

The funding of this work by the German Research Foundation (DFG) is gratefully acknowledged.